A joint *Fermi*-LAT and H.E.S.S. analysis of the Crab nebula

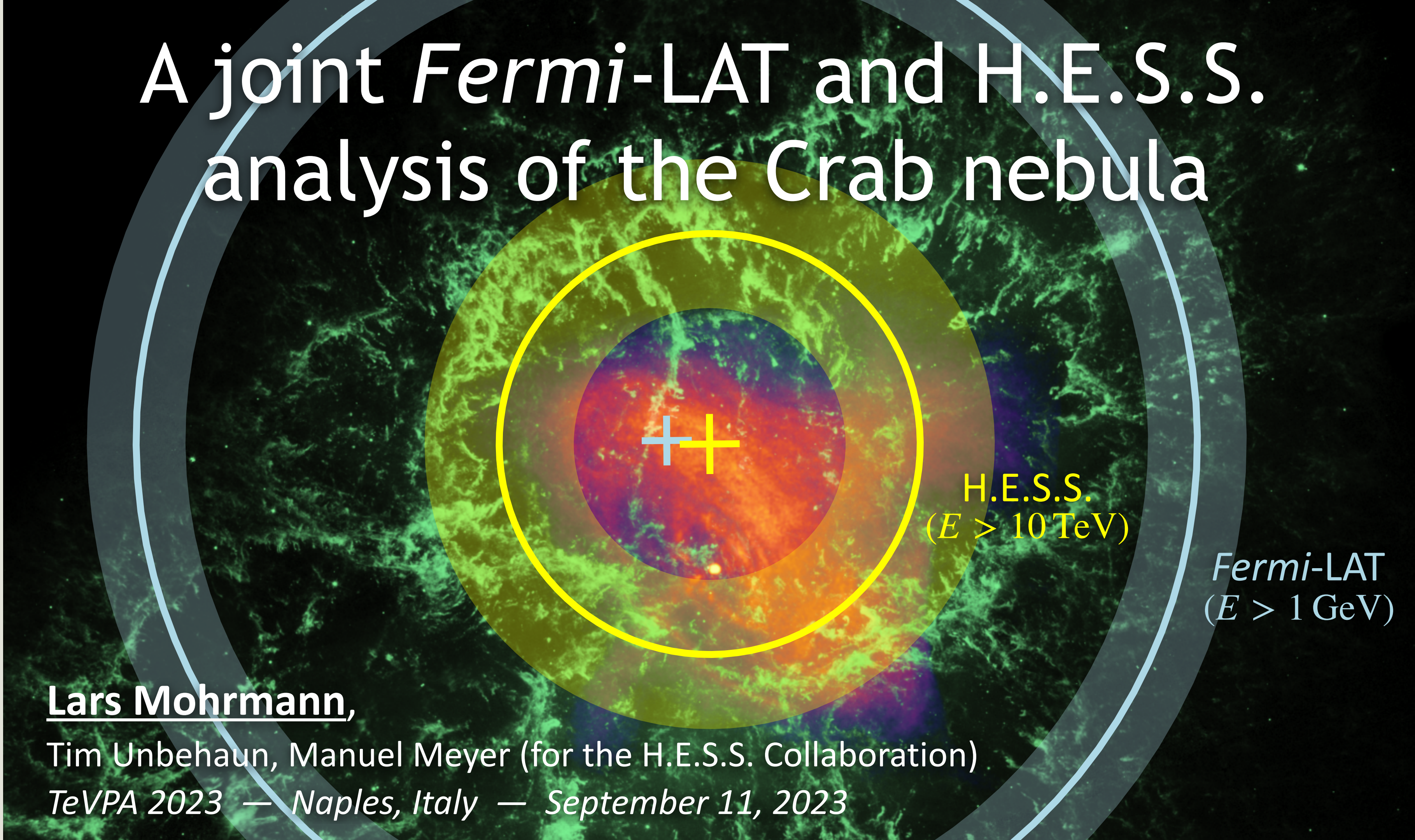

Lars Mohrmann,
Tim Unbehaun, Manuel Meyer (for the H.E.S.S. Collaboration)
MAX-PLANCK-INSTITUT FÜR KERNPHYSIK

TeVPA 2023 — Naples, Italy — September 11, 2023

The Crab nebula

- Probably the best-studied high-energy gamma-ray source
- The archetype of a pulsar wind nebula
- Visible across the electromagnetic spectrum
- Emission mostly non-thermal radiation from relativistic electrons

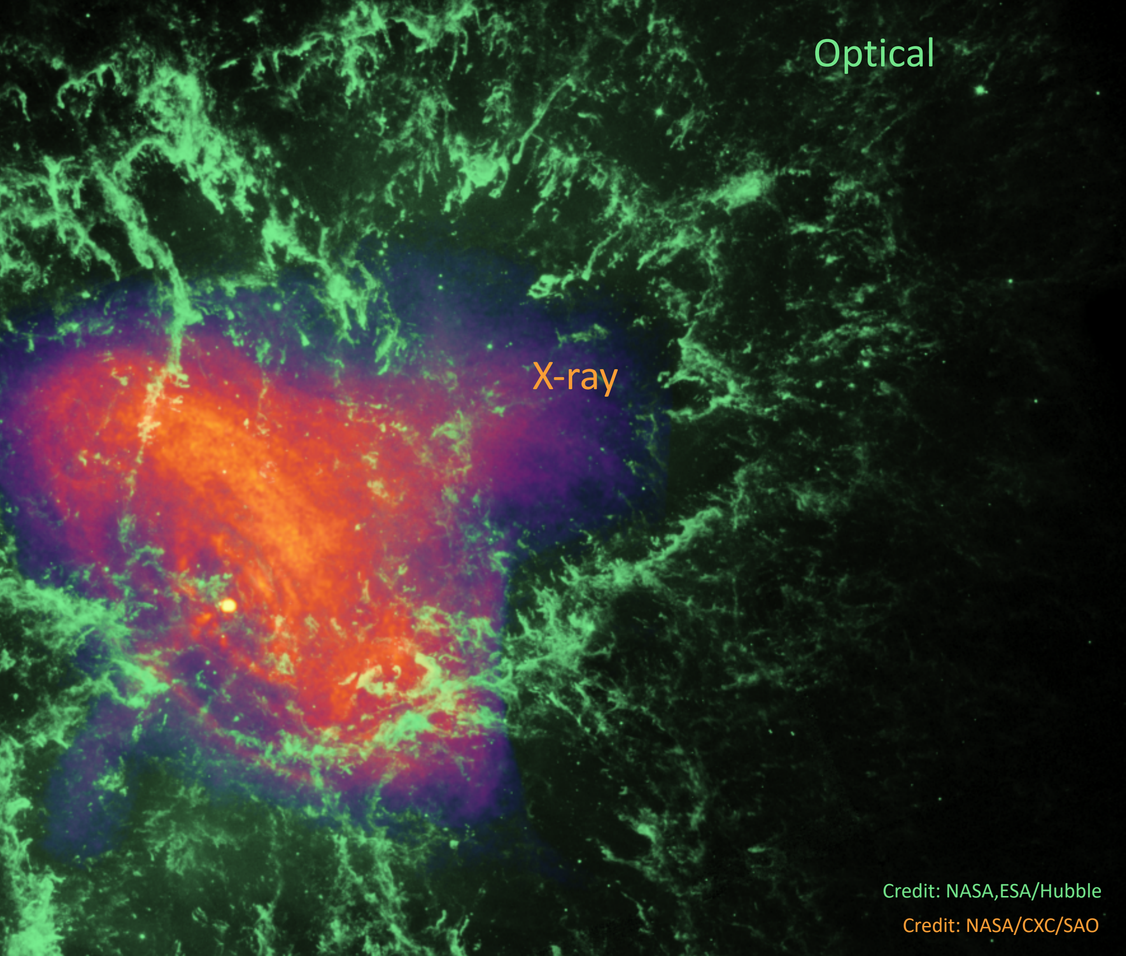

Credit: NASA,ESA/Hubble

Credit: NASA/CXC/SAO

MAX-PLANCK-INSTITUT FÜR KERNPHYSIK

The Crab nebula SED

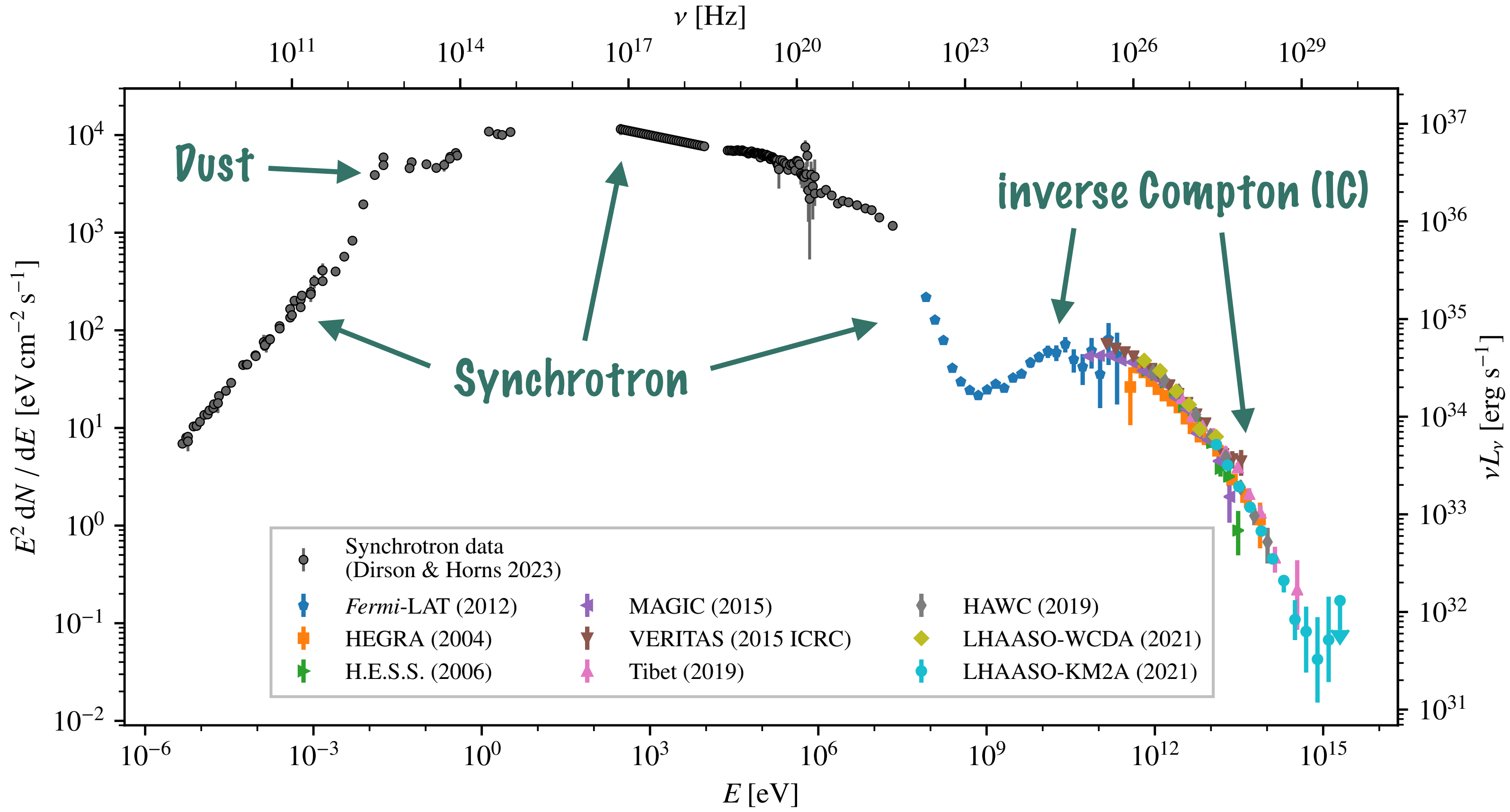

Extension of the IC component

- At GeV energies (with *Fermi*-LAT)

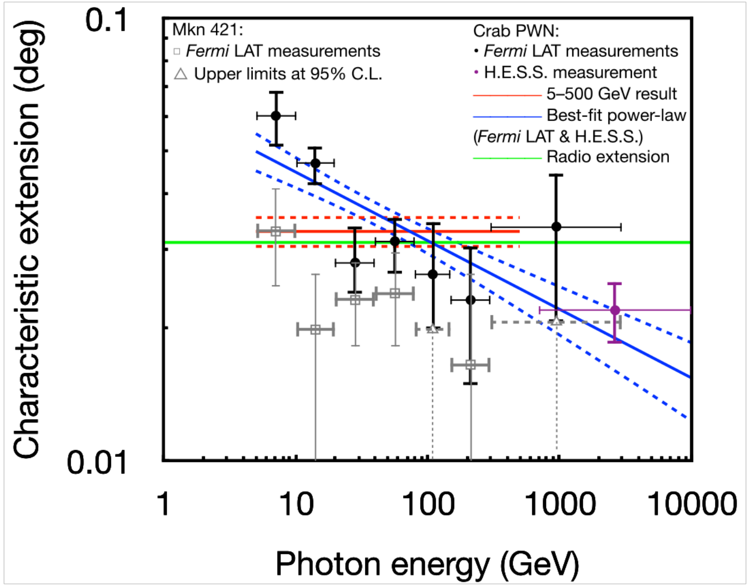

[Yeung & Horns, ApJ **875**, 123 (2019)]

- At TeV energies (with H.E.S.S.)

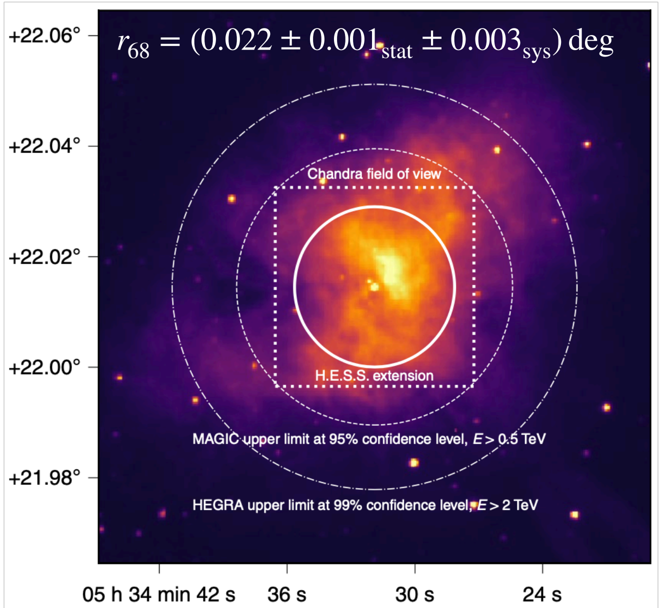

[HESS Coll., Nat. Astron. **4**, 167 (2020)]

Extension of the IC component

- At GeV energies (with *Fermi*-LAT)

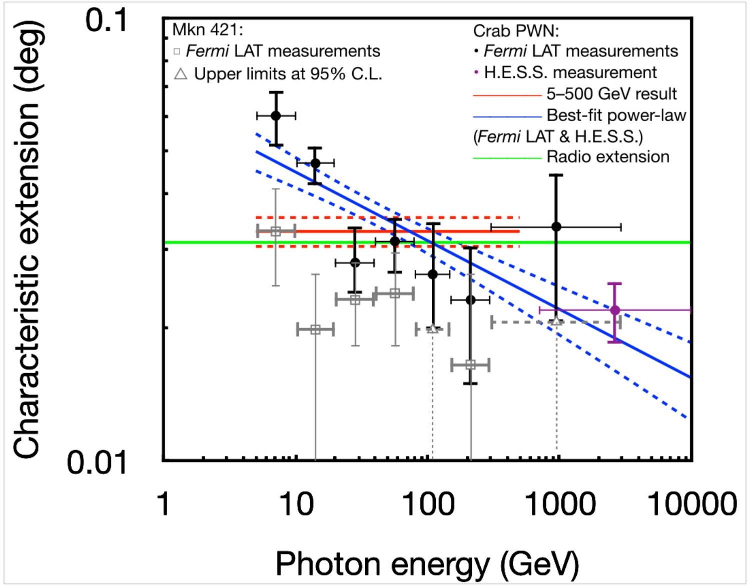

[Yeung & Horns, ApJ **875**, 123 (2019)]

- At TeV energies (with H.E.S.S.)

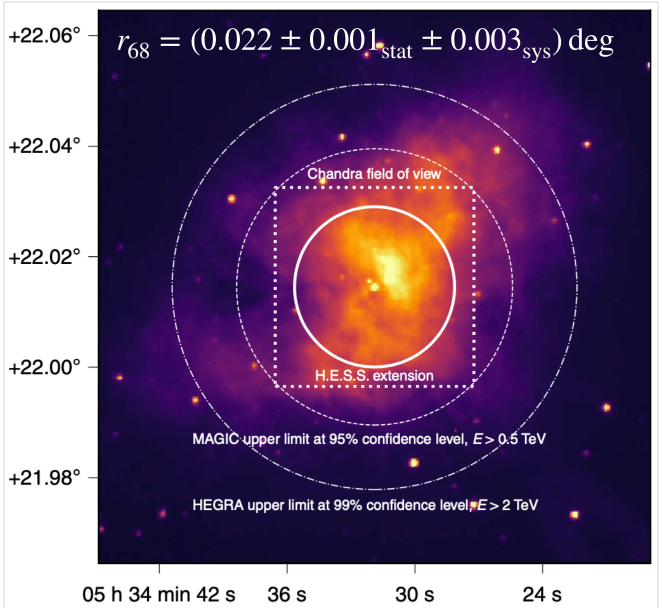

[HESS Coll., Nat. Astron. **4**, 167 (2020)]

- *Missing so far: self-consistent analysis of spectrum & extension across entire gamma-ray domain*

Joint *Fermi*-LAT and H.E.S.S. analysis

- *Fermi*-LAT
  - 11.4 years of data
  - $1\,\mathrm{GeV} < E < 1\,\mathrm{TeV}$
  - phase-resolved analysis to remove contamination from Crab pulsar

- H.E.S.S.
  - 50 h of "stereo" data $\rightarrow$ $E > 560\,\mathrm{GeV}$
  - 30 h of "mono" data $\rightarrow$ $E > 240\,\mathrm{GeV}$

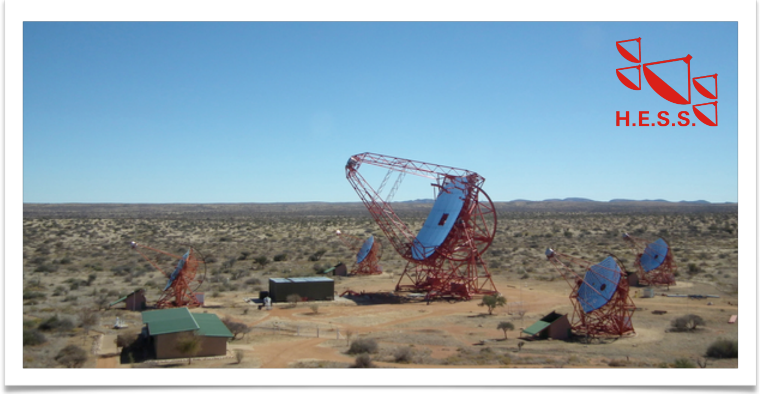

- Joint spectral + morphological analysis with $\gamma\pi$ A **Python** package for **gamma-ray** astronomy
  - measure spectrum & extension from 1 GeV to > 10 TeV
  - constrain phenomenological emission models

Results of *Fermi*-LAT-only analysis

- Energy spectrum
  - synchrotron component fitted in first iteration, then fixed
  - fit of IC component performed with Fermipy and Gammapy
    - perfect agreement between tools
    - validation of *Fermi*-LAT data analysis with Gammapy

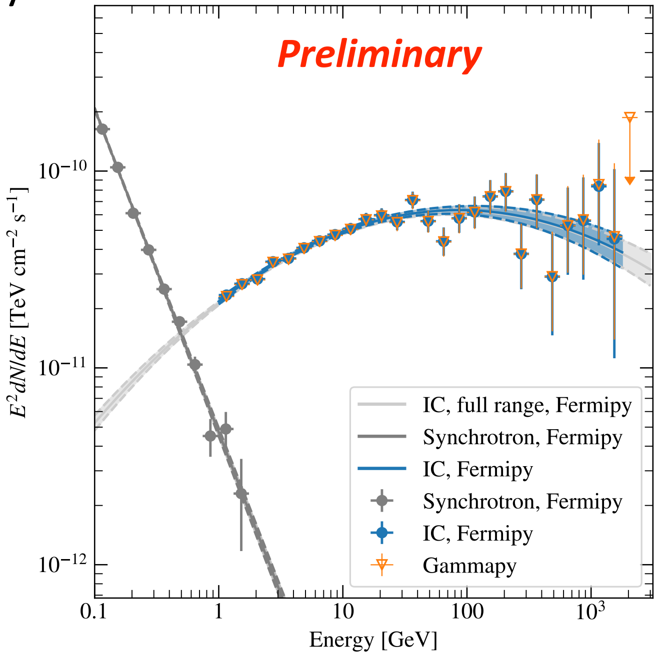

- Extension
  - Gaussian spatial model
  - $r_{68} = (2.22 \pm 0.18_{\mathrm{stat}}\,{}^{+0.54}_{-0.48}\,\mathrm{sys})'$
    - compatible with literature value

      $r_{68} = (1.80 \pm 0.18_{\mathrm{stat}} \pm 0.42_{\mathrm{sys}})'$

      (Ackermann et al. 2018, ApJS 237, 32)

Results of H.E.S.S.-only analysis

- Energy spectrum
  - derive flux points for mono and stereo data
    → nicely compatible
  - good agreement with literature spectra

- Extension (stereo data only)
  - Gaussian spatial model
  - $r_{68} = (1.62 \pm 0.05_{\mathrm{stat}}\ {}^{+0.21}_{-0.24}{}_{\mathrm{sys}})'$
    - small tension with literature value
      $r_{68} = (1.30 \pm 0.07_{\mathrm{stat}} \pm 0.17_{\mathrm{sys}})' \quad (E > 700\,\mathrm{GeV})$
      (H. Abdalla et al. 2020, Nat. Astron. 4, 167)

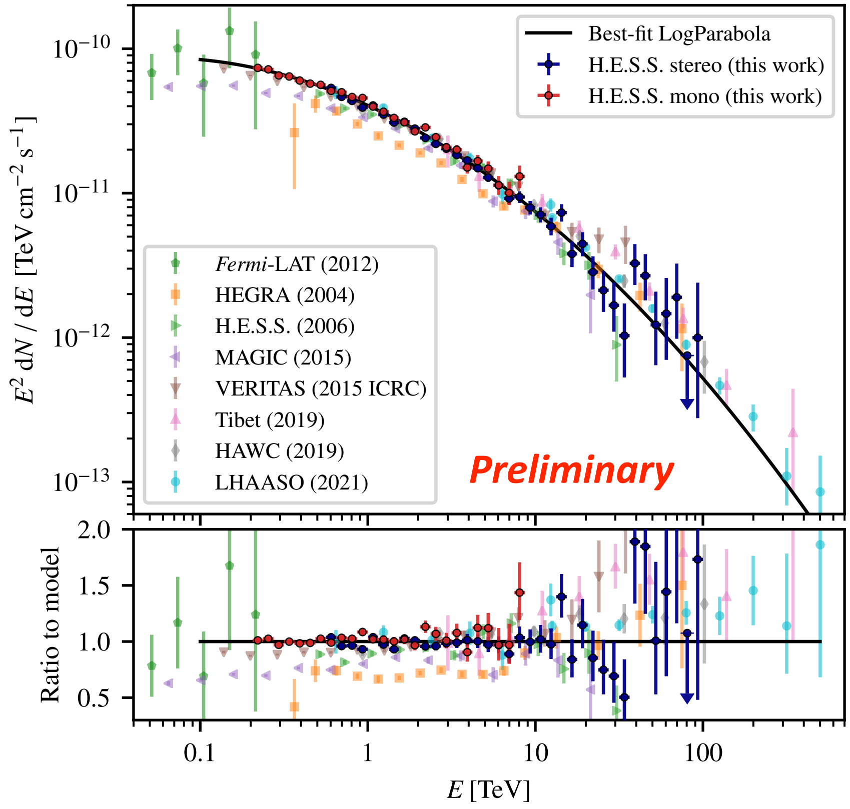

Joint analysis — extension measurement

- Joint fit of *Fermi*-LAT and H.E.S.S. stereo data
- Model spectrum with smoothly broken power law
- Measure extension in energy bands
  → strong indication for nebula continuously shrinking with energy

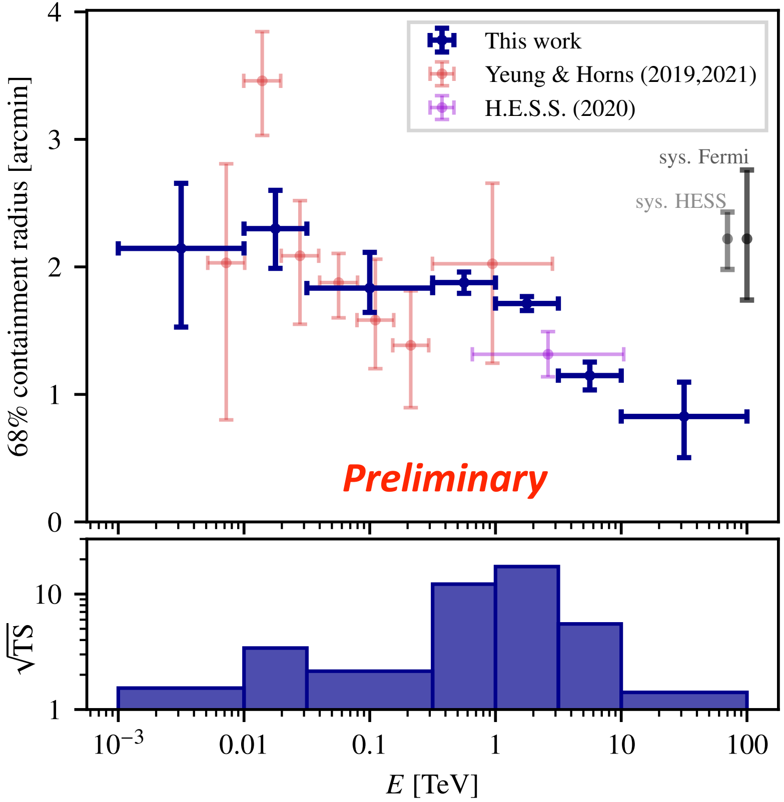

Joint analysis — extension measurement

- Joint fit of *Fermi*-LAT and H.E.S.S. stereo data
- Model spectrum with smoothly broken power law
- Measure extension in energy bands
  → strong indication for nebula continuously shrinking with energy

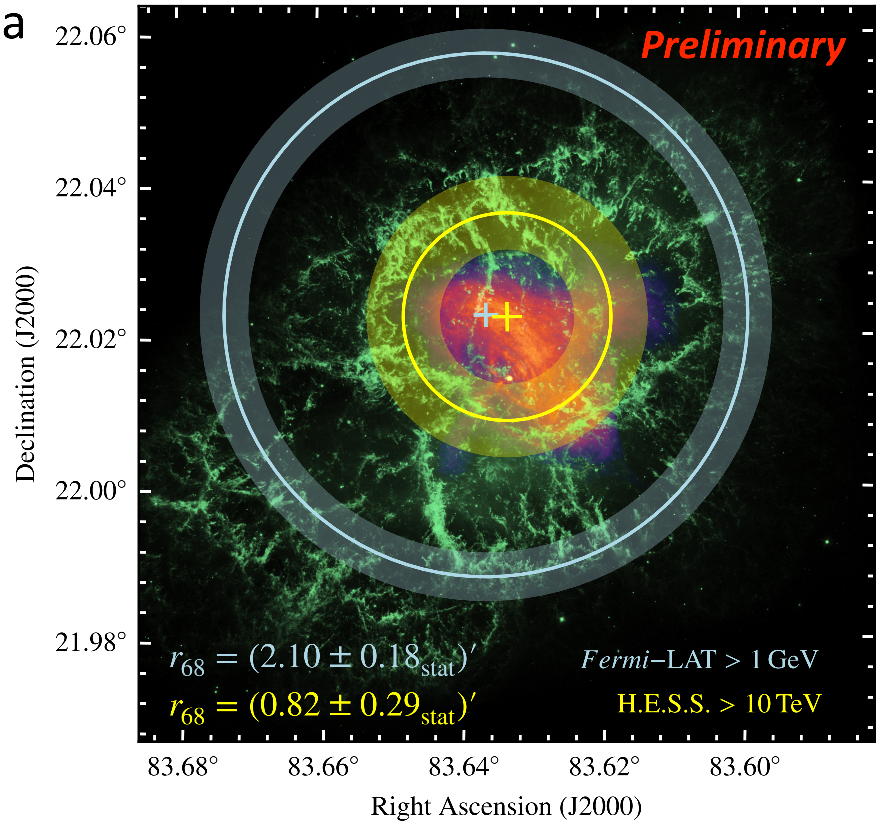

Joint analysis — modelling

- Three static, radially symmetric synchrotron self-Compton (SSC) models
- All models consider two electron populations:
  - relic "radio" electrons
    - fill entire nebula
    - spatial distribution constant with energy
  - freshly injected "wind" electrons
    - accelerated at standing shock
    - spatial distribution changes with energy
- Radial dependence of *B* field:
  - "constant *B*-field model"
    → *B* constant throughout nebula
  - "variable *B*-field model"
    → *B* field decreases as $r^{-\alpha}$
  - "Kennel & Coroniti model"
    → MHD flow model (includes particle transport)

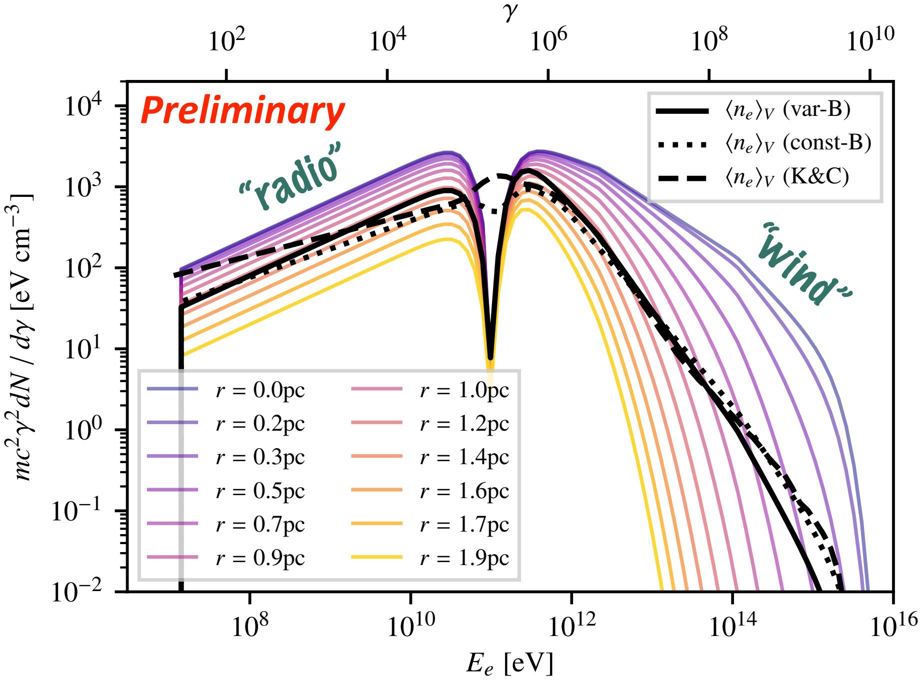

Joint analysis — modelling

- Three static, radially symmetric synchrotron self-Compton (SSC) models
- All models consider two electron populations:
  - relic "radio" electrons
    - fill entire nebula
    - spatial distribution constant with energy
  - freshly injected "wind" electrons
    - accelerated at standing shock
    - spatial distribution changes with energy
- Radial dependence of *B* field:
  - "constant *B*-field model"
    - → *B* constant throughout nebula
  - "variable *B*-field model"
    - → *B* field decreases as $r^{-\alpha}$
  - "Kennel & Coroniti model"
    - → MHD flow model (includes particle transport)

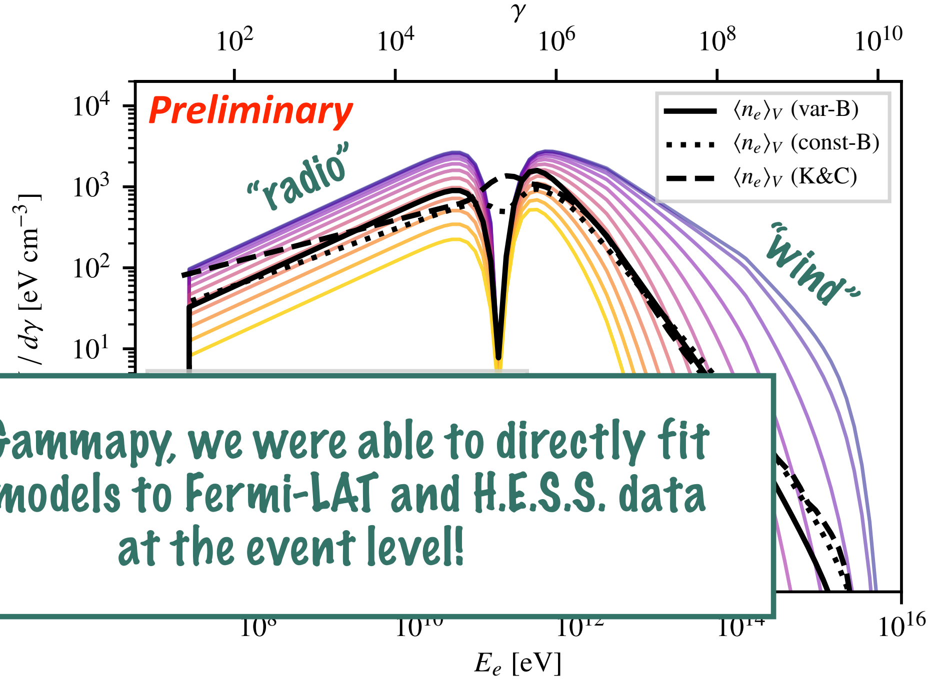

With Gammapy, we were able to directly fit these models to Fermi-LAT and H.E.S.S. data at the event level!

Modelling results

- Include constraints from synchrotron flux and extension measurements:
  $C_{\mathrm{tot}} = -2 \ln \mathcal{L}_{\mathrm{tot}} = C_{\mathrm{IC}} + \chi^2_{\mathrm{SYN,flux}} + \chi^2_{\mathrm{SYN,ext}}$
- "Variable B-field model" yields best fit (statistically highly preferred)
- All models predict shrinking extension of electron distribution with energy

Model	ΔC_{tot}	ΔC_{IC}	$\chi^2_{\mathrm{SYN,flux}}$ (#)	$\chi^2_{\mathrm{SYN,ext}}$ (#)	N_{par}	ΔAIC
variable B-field model	0	0	152.7 (194)	60.3 (14)	16	0
constant B-field model	374.0	264.1	246.0 (194)	76.9 (14)	15	372.0
Kennel & Coroniti	292.6	143.0	285.5 (194)	77.1 (14)	12	284.6

Preliminary

Modelling results

- Include constraints from synchrotron flux and extension measurements:
  $$C_{\rm tot} = -2\ln\mathcal{L}_{\rm tot} = C_{\rm IC} + \chi^2_{\rm SYN,flux} + \chi^2_{\rm SYN,ext}$$
- "Variable B-field model" yields best fit (statistically highly preferred)
- All models predict shrinking extension of electron distribution with energy

Electron extension vs energy:

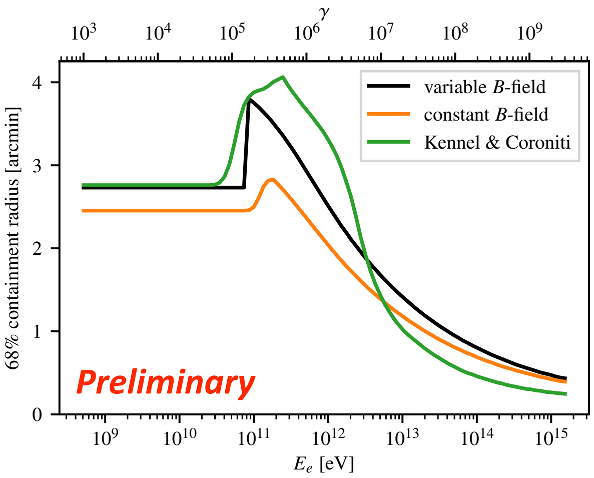

B-field vs radius:

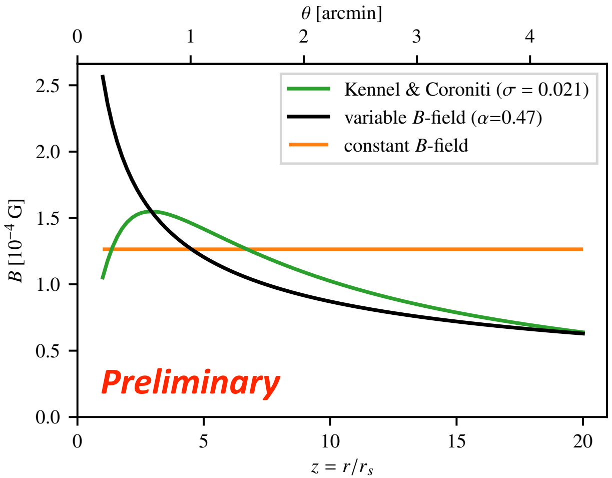

Intensity vs radius:

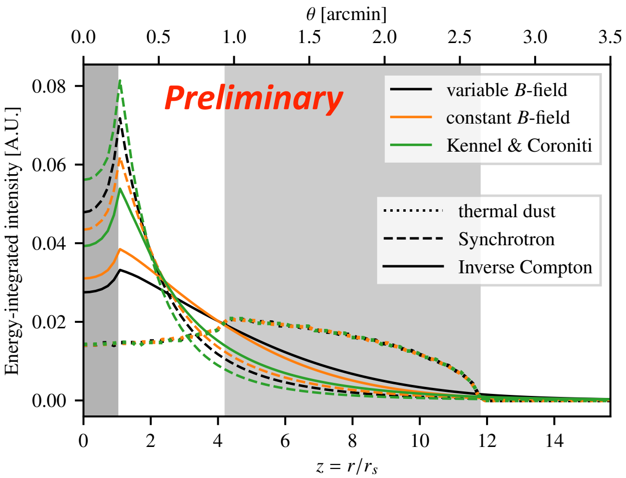

SED with best-fit models

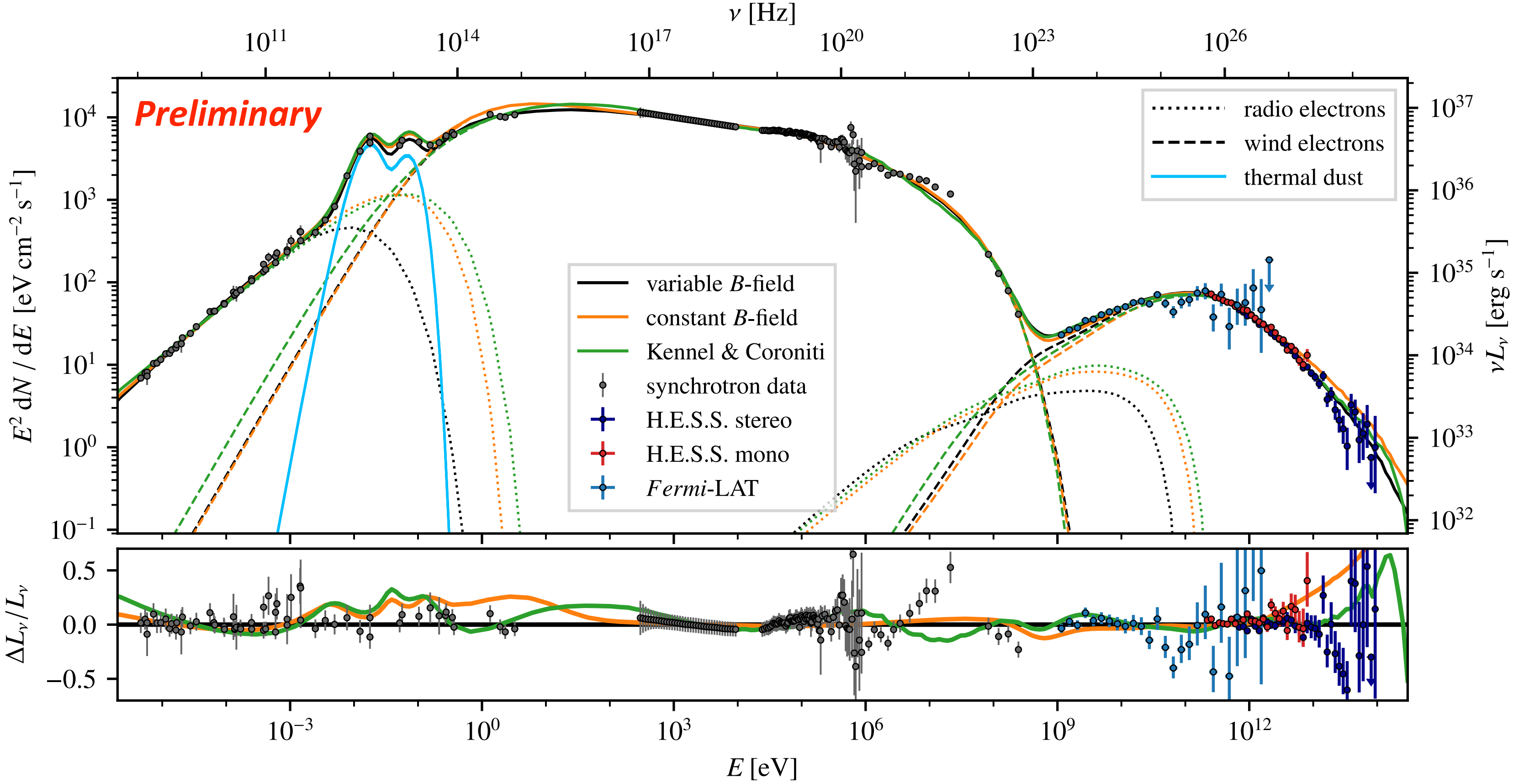

SED with best-fit models

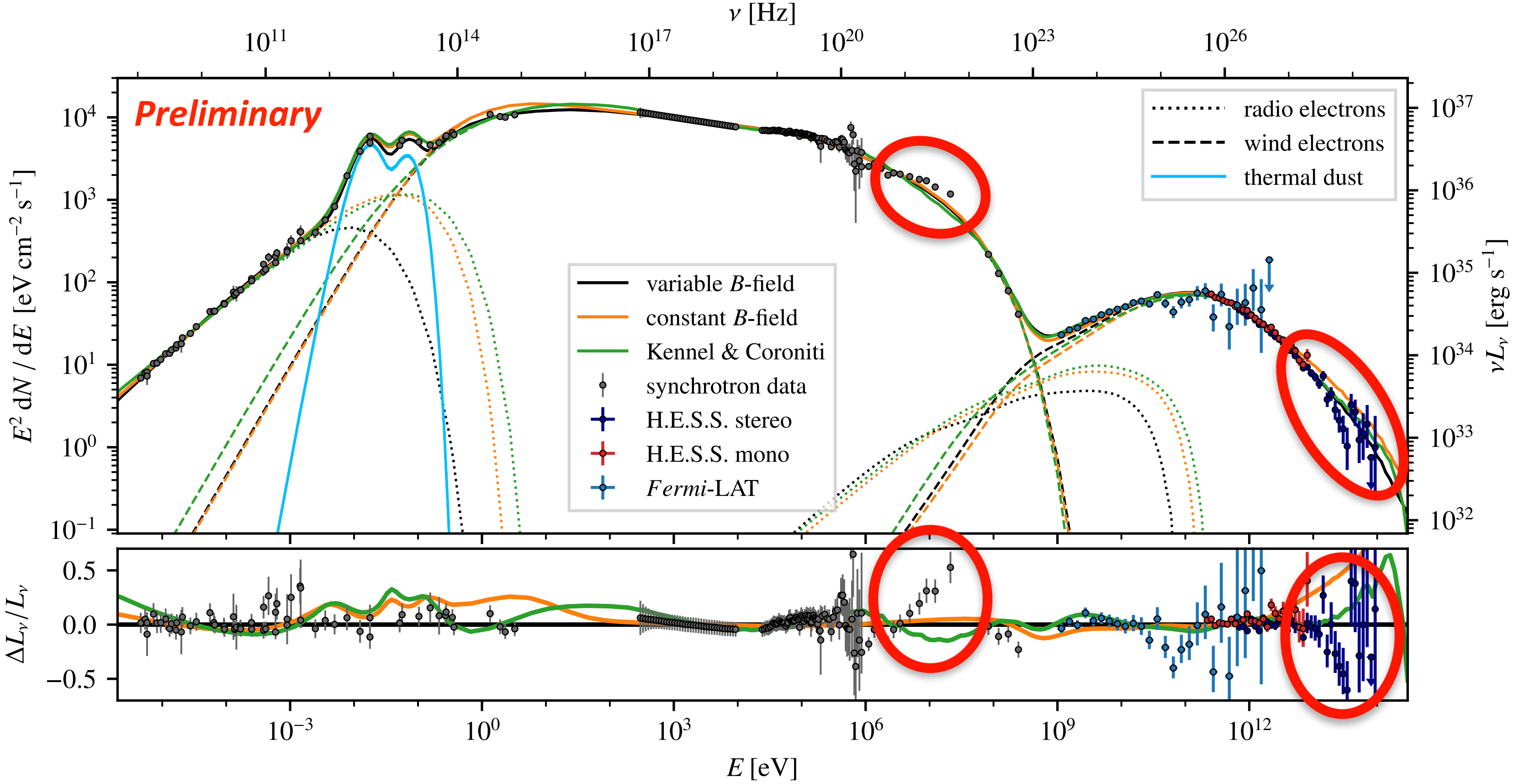

IC part with best-fit models

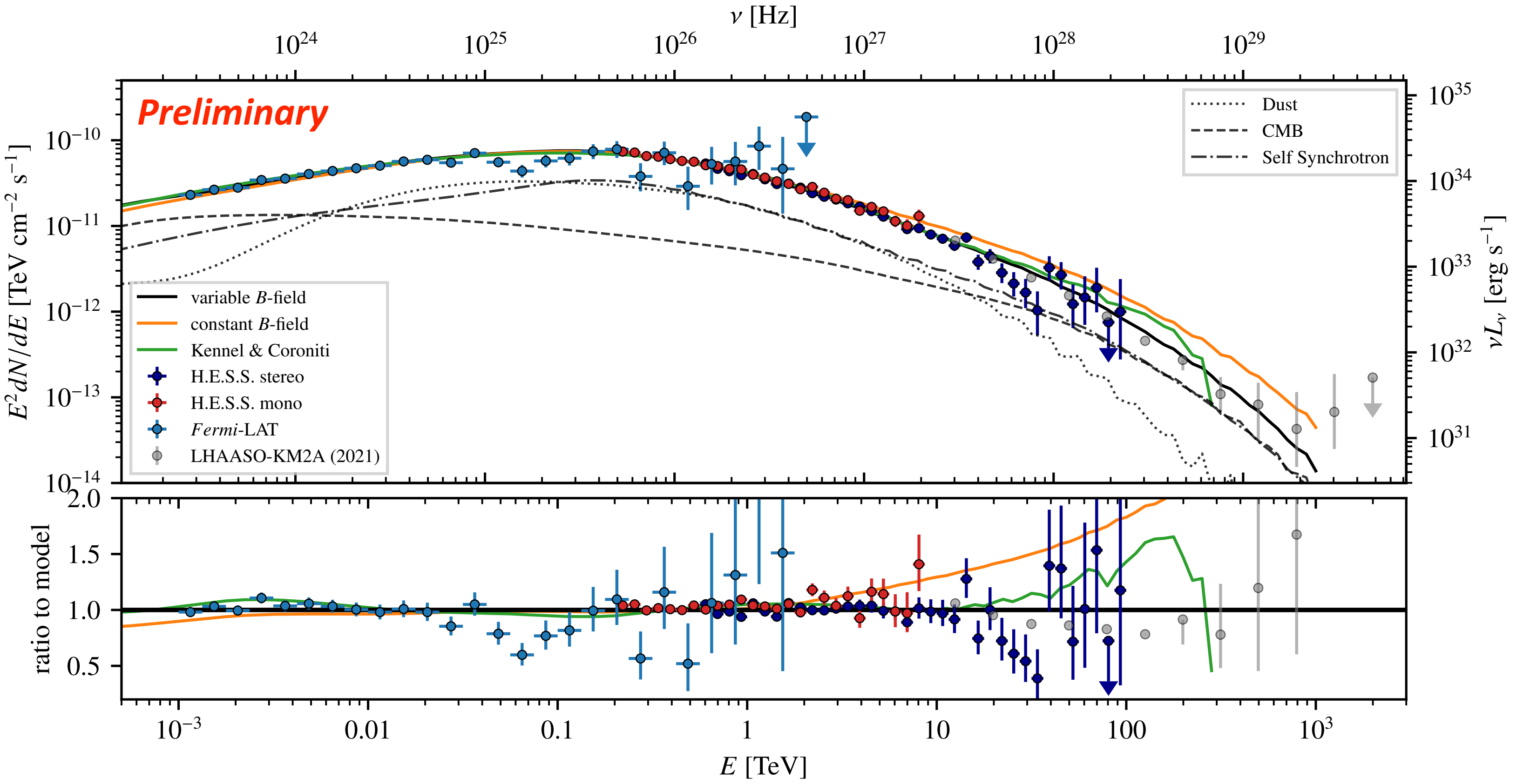

IC part with best-fit models

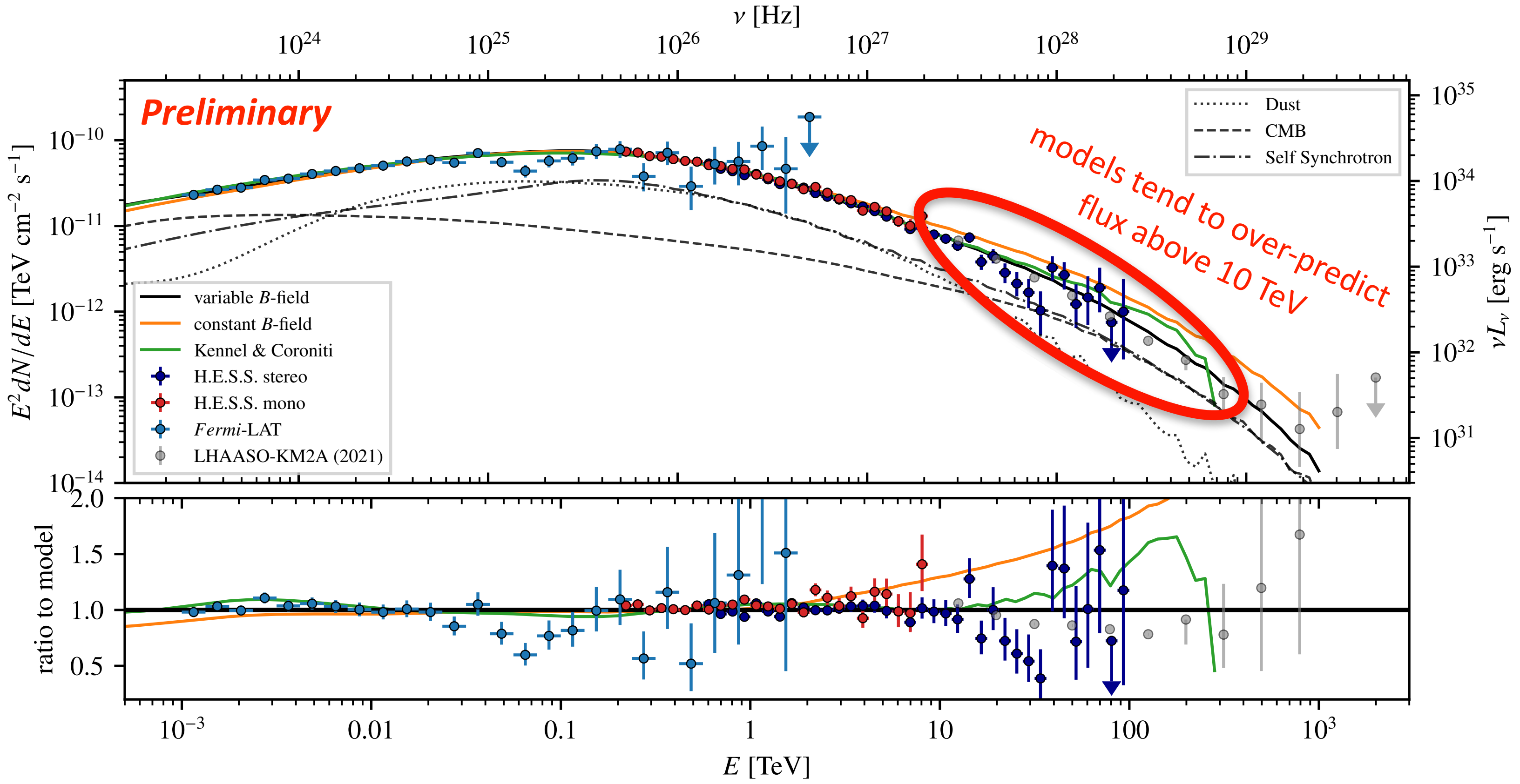

Extension with best-fit models

- Small X-ray extension in conflict with too large extension of IC nebula

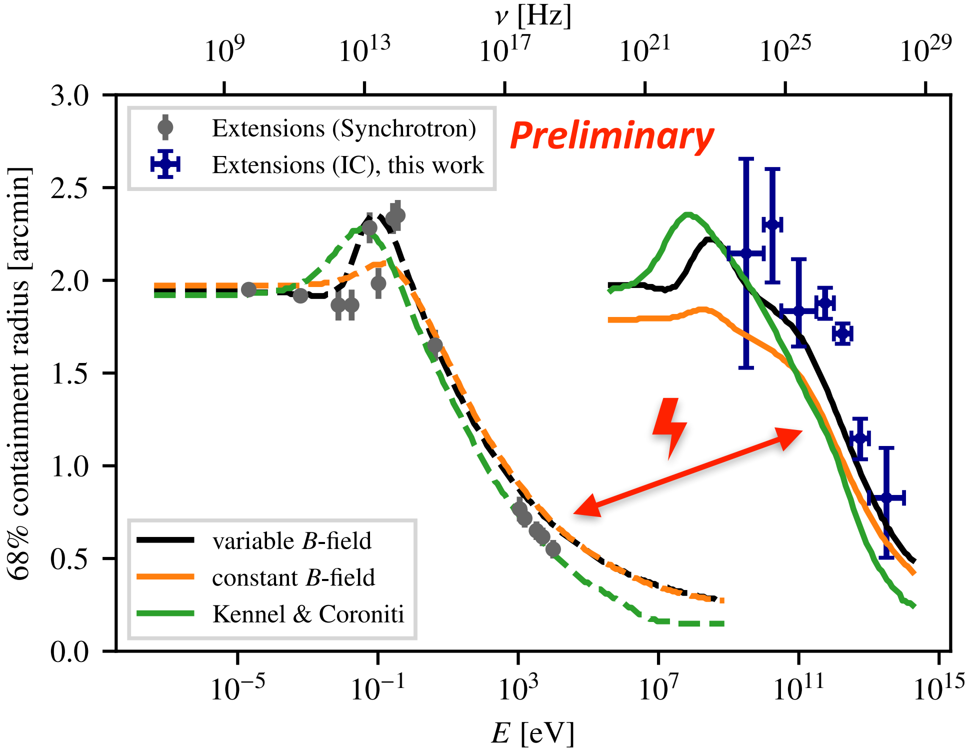

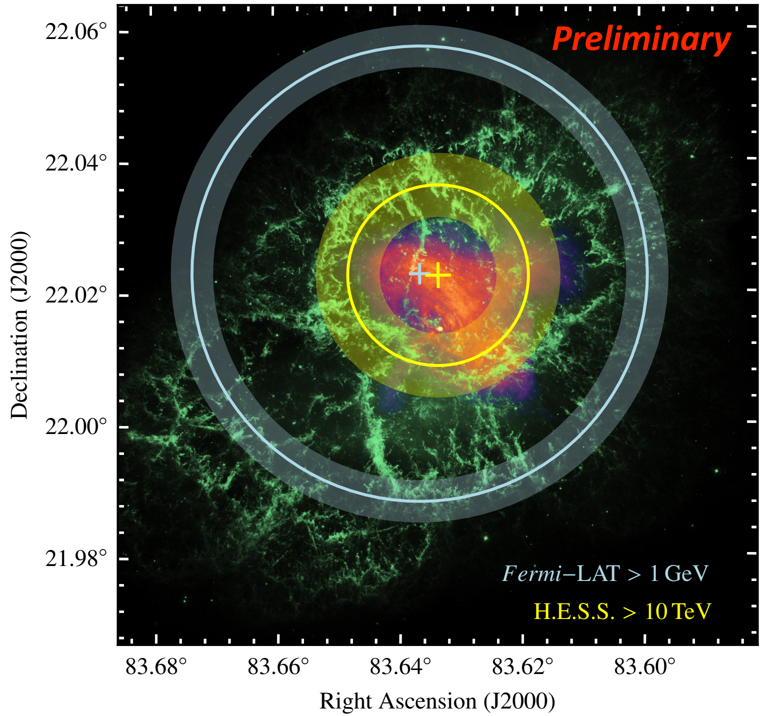

Model maps

- Shown for the "variable B-field model"

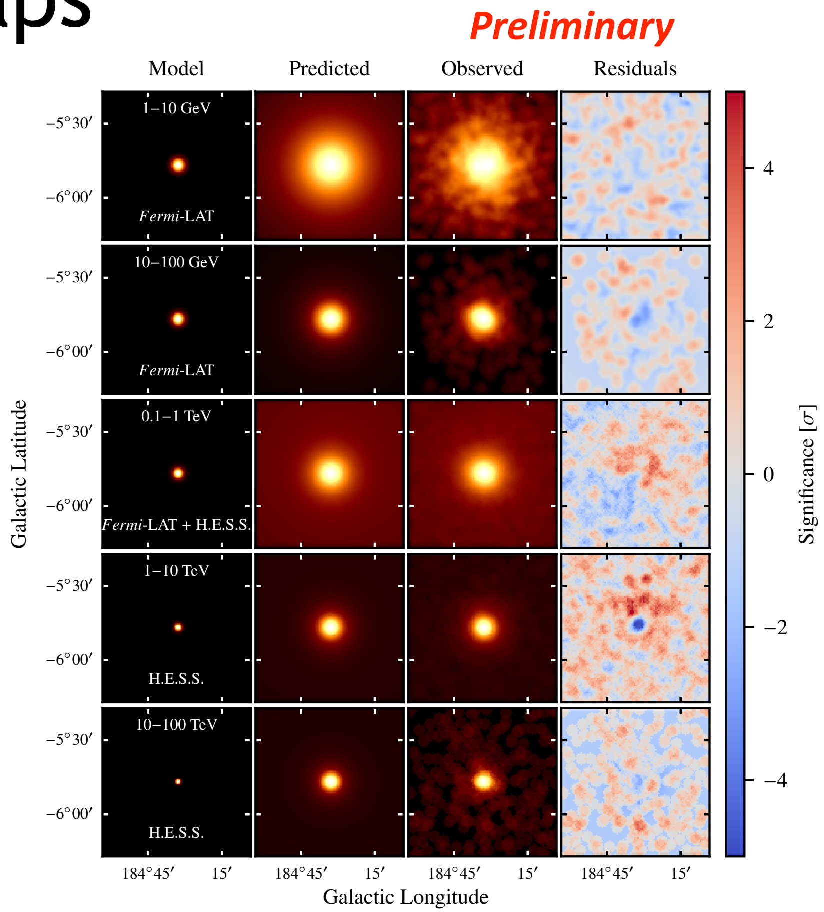

Model maps

- Shown for the “variable B-field model”
- Residuals between 1 TeV and 10 TeV
  → predicted extension too small

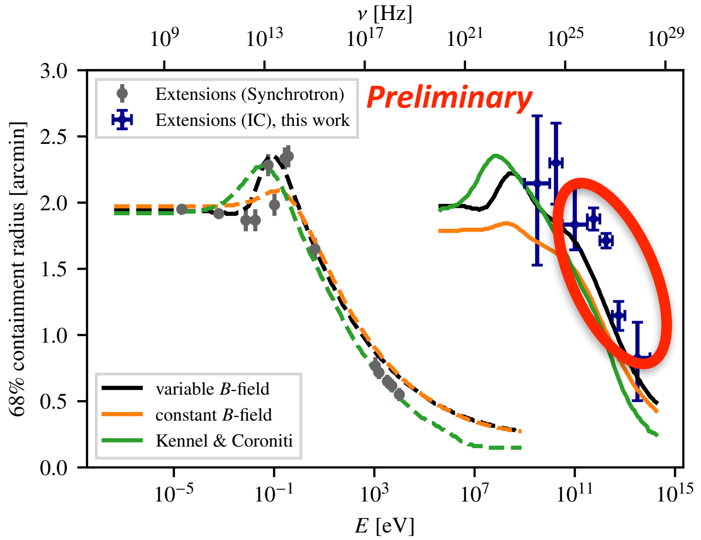

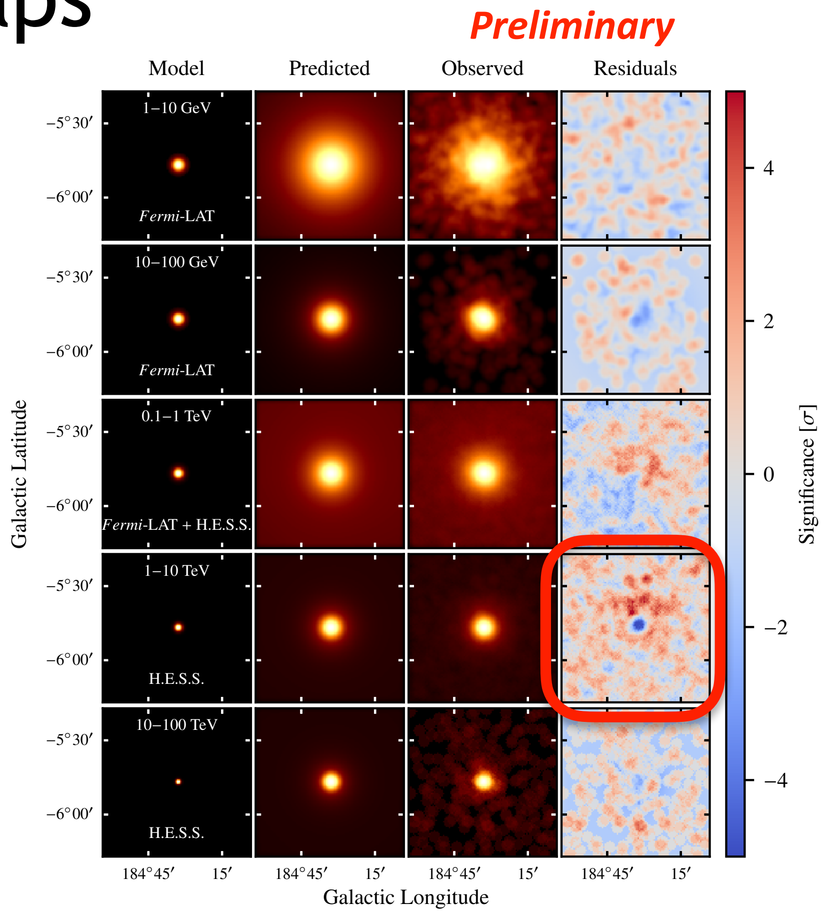

Conclusion

- Joint *Fermi*-LAT and H.E.S.S. analysis of Crab nebula
  - measure spectrum & extension from 1 GeV to > 10 TeV
  - constrain phenomenological emission model

- Main results
  - strong indication for nebula shrinking with energy
  - none of tested models can fully describe MWL data (spectrum + extension)

- Publication currently under Collaboration review

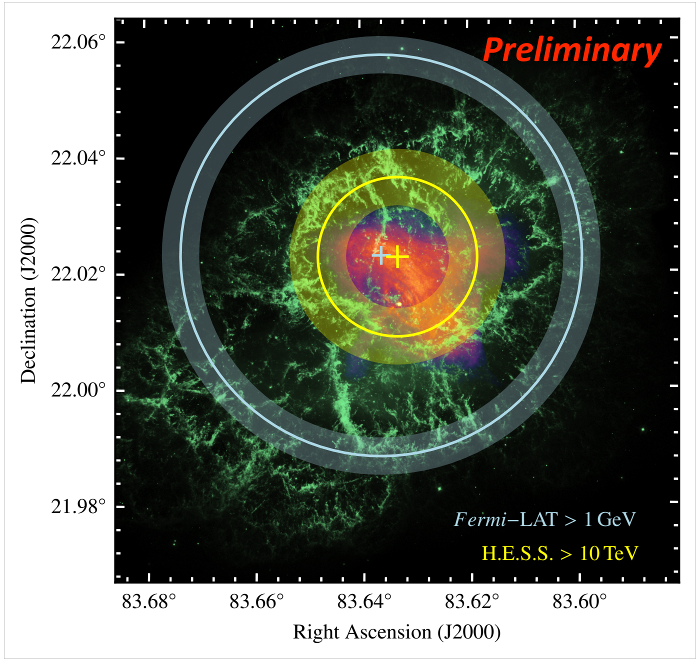

Backup slides

Fermi-LAT analysis details

- Data selection
  - time range: Aug 4, 2008 — Jan 4, 2020
  - P8R3_SOURCE event class
  - select events in "Off" phase of pulsar
- Initial modelling
  - energy range: 100 MeV — 3 TeV
  - region of interest: 10°x10°, spatial pixel size: 0.04°
  - fit both synchrotron and IC component
- Final modelling
  - energy range: 1 GeV — 1.78 TeV
  - region of interest: 6°x6°, spatial pixel size: 0.025°
  - event types: PSF0, PSF1, PSF2, PSF3
  - keep synchrotron component fixed

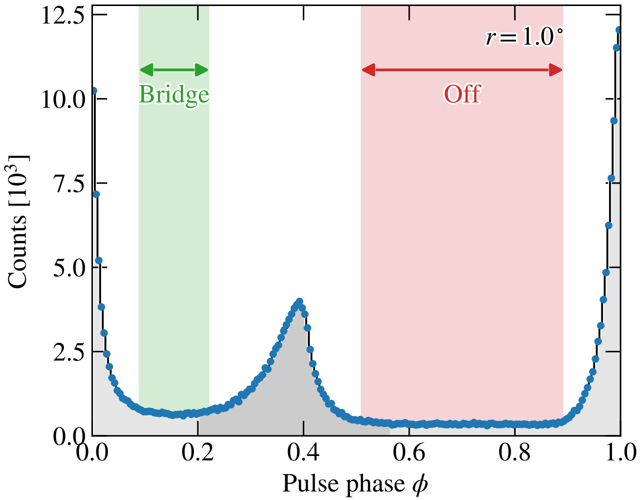

Detailed *Fermi*-LAT analysis settings

Parameter	Selection > 100 MeV	Selection > 1 GeV
Time range	11.5 years	11.5 years
Energy range	> 100 MeV	> 1 GeV
ROI size	10º x 10º	6º x 6º
Pulse phase	0.51 < phase < 0.89	0.51 < phase < 0.89
Max. Zenith angle	90º	100º
Filter	DATA_QUAL>0 && LAT_CONFIG==1	DATA_QUAL>0 && LAT_CONFIG==1
Spatial binning (exp)	0.04º / pixel	0.025º / pixel
Spatial Binning (LT)	1º / pixel	0.025º / pixel
Energy binning	8 bins per decade	8 bins per decade
Event Class / IRFs	P8R3_SOURCE_V2	P8R3_SOURCE_V2
Event types	FRONT + BACK	PSF 0, PSF1, PSF2, PSF3
Catalog	4FGL	4FGL

Fermi-LAT TS and residual maps for *E*>100 MeV

- Flat residuals and no indication for additional sources

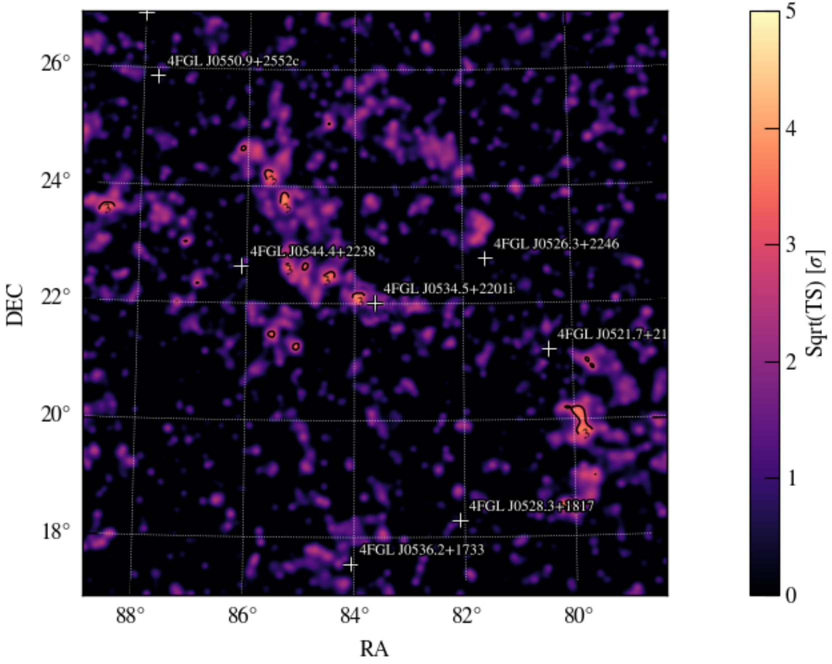

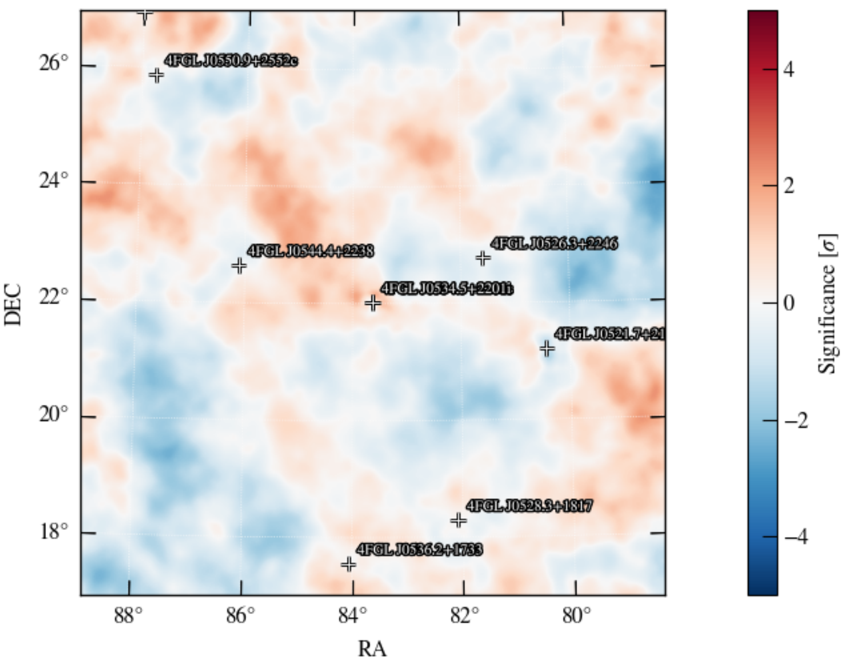

Fermi-LAT TS and residual maps for *E*>1 GeV

- Flat residuals and no indication for additional sources

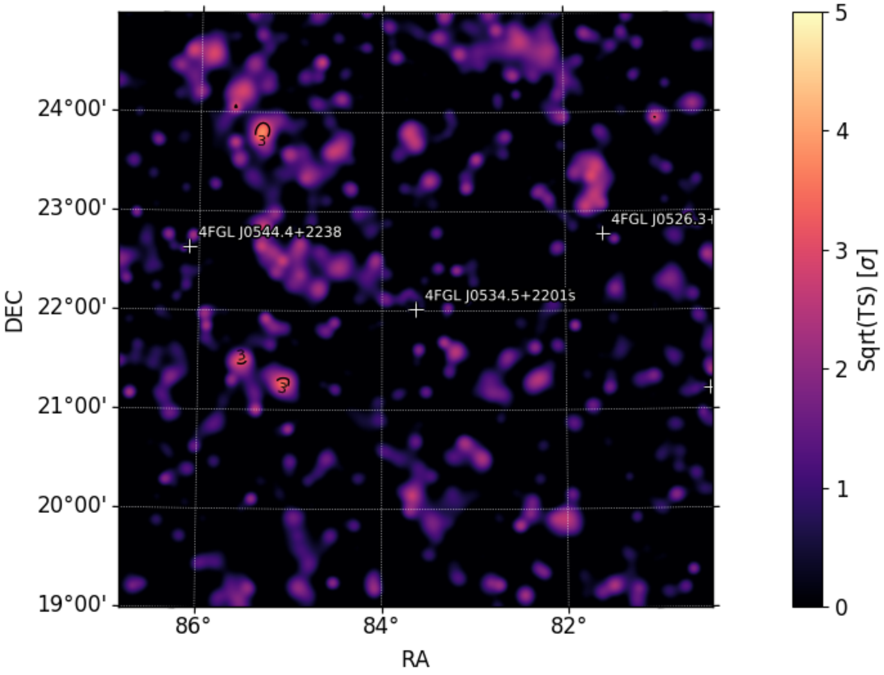

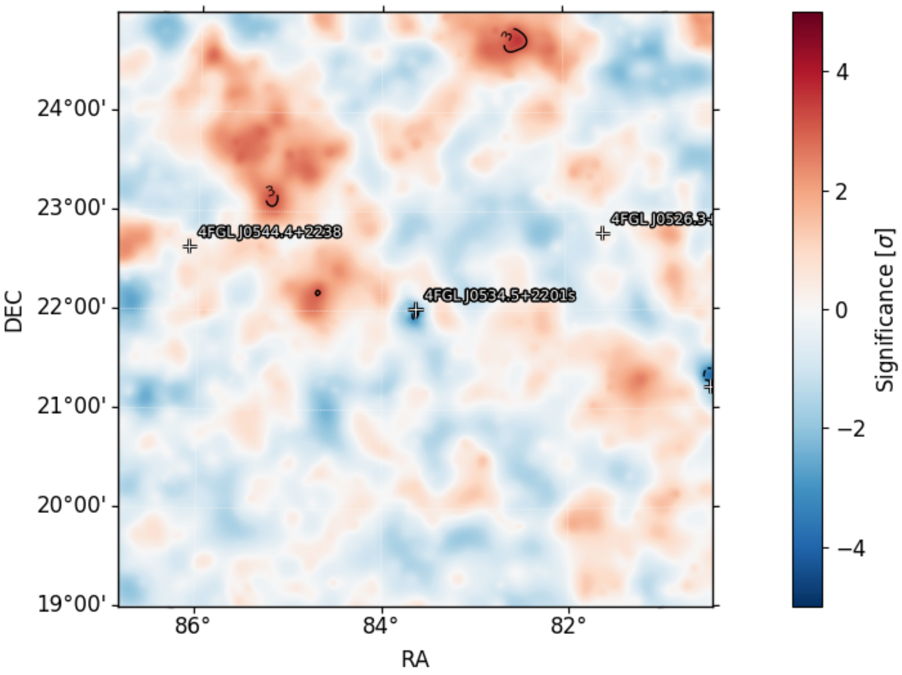

Fermi-LAT extension analysis

- Carried out with fermipy extension module
- Diffuse background normalisations and source position left free during fit
- Extension consistent with Ackermann et al. (2018) (90 months of data)

	Dec (deg)	RA (deg)	TS ext	TS ext PSF hi	TS ext PSF lo	Extension = R_{68} (deg)
Gauss	22.032 +/- 0.011	83.626 +/- 0.011	47.6	16.3	110.7	$0.037 \pm 0.003_{stat} + 0.009_{sys} - 0.008_{sys}$
Disk	22.032 +/- 0.008	83.626 +/- 0.009	47.6	16.3	107.7	$0.038 + 0.005_{stat} - 0.002_{stat} \pm 0.008_{sys}$

$$\sigma = -\frac{R_{68}}{\sqrt{-2\ln(1-0.68)}} = 0.0245^\circ \pm 0.0020^\circ$$

Fermi-LAT energy-dependent extension

- 8 bins per decade

Gaussian

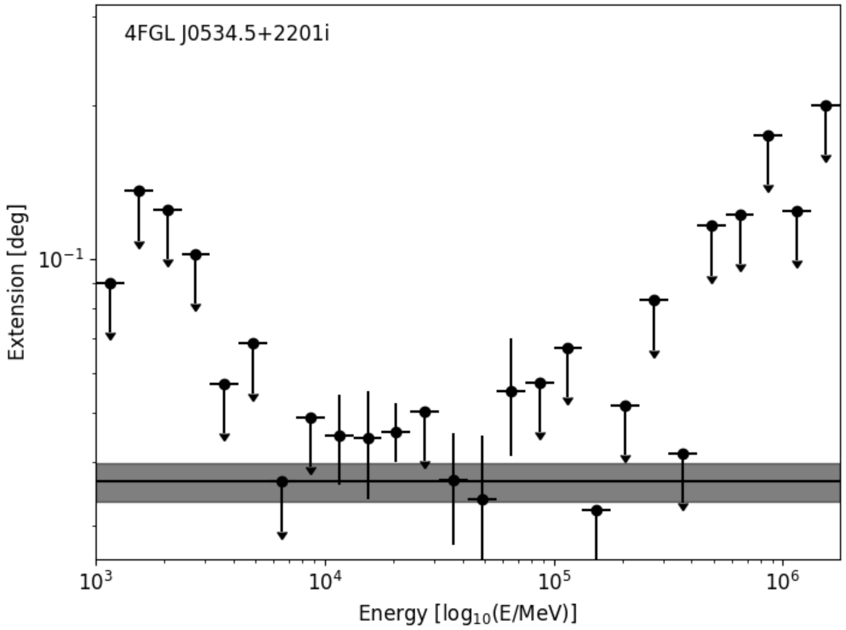

Disk

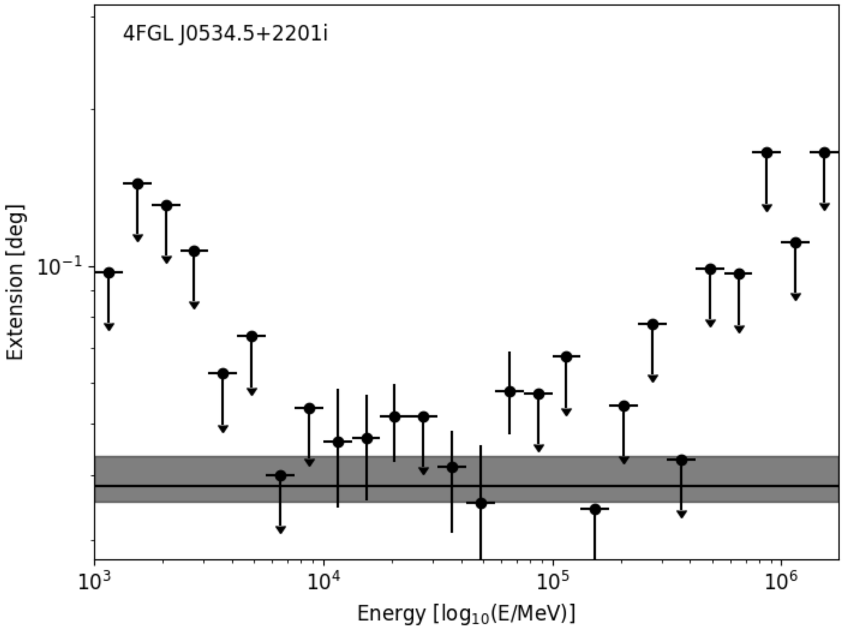

Fermi-LAT energy-dependent extension

- 2 bins per decade

Gaussian

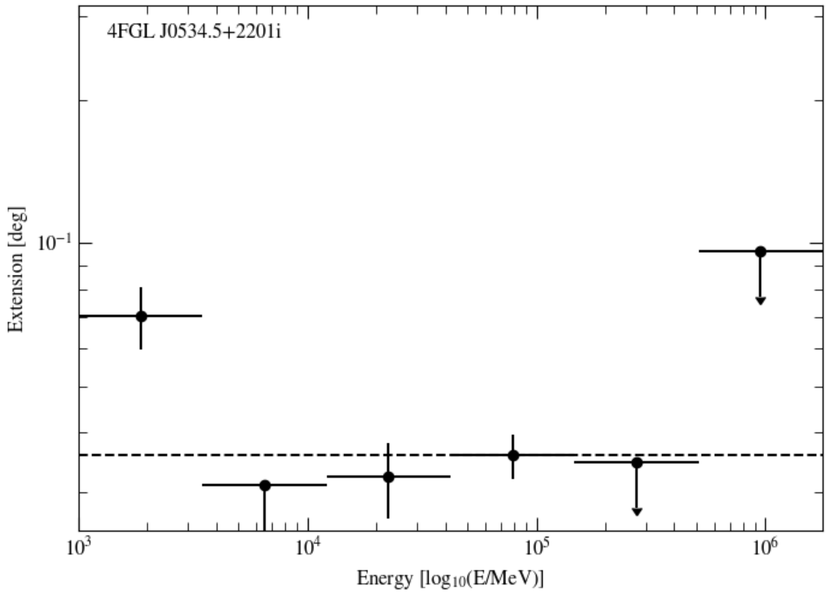

Disk

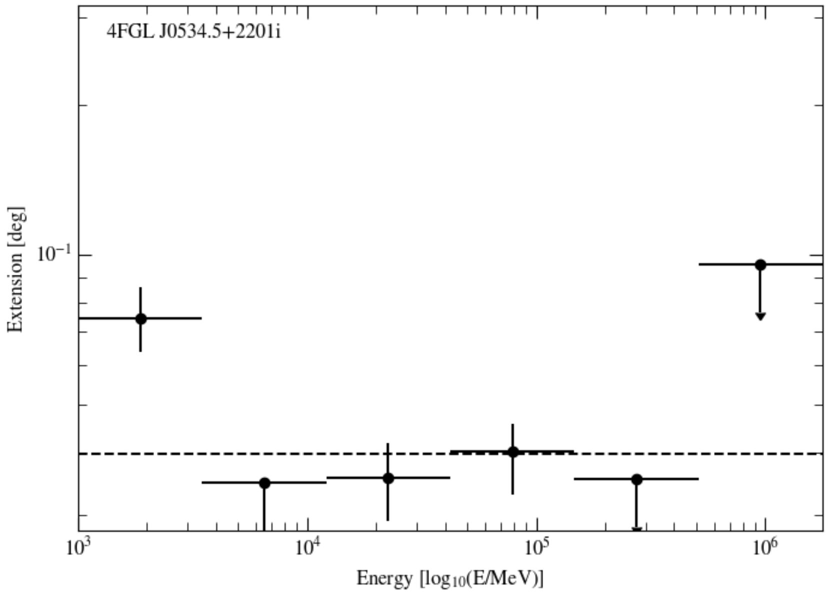

H.E.S.S. analysis details

- Data sets
  - stereo (CT1-4)
    - 2004–2015
    - analysis configuration: “std_ImPACT_3tel”
    - threshold: 560 GeV
  - mono (CT5-FlashCam)
    - 2019–2021
    - analysis configuration: “safe_zeta_mono”
    - threshold: 240 GeV
- Following quality selection of first extension paper
  - e.g. zenith angle < 55°, offset angle < 1°
- 3D likelihood analysis with background model

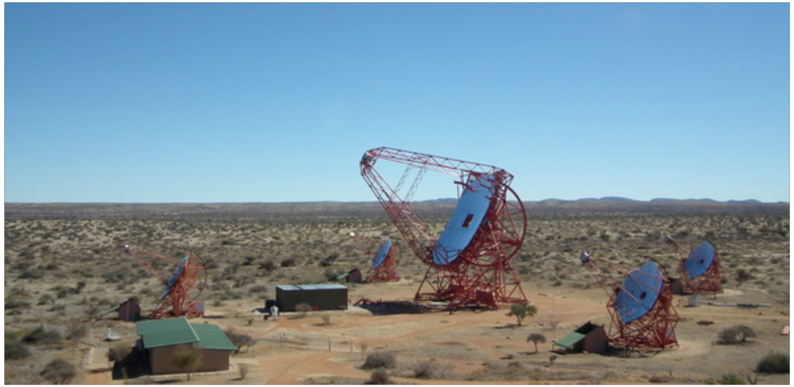

Data set	Year	Runs	Livetime (h)
stereo	2004	18	7.82
	2005	6	2.81
	2007	5	2.34
	2008	4	1.43
	2009	10	4.69
	2013	58	25.19
	2014	7	3.01
	2015	6	2.80
mono	2019	18	8.41
	2020	42	19.44
	2021	5	2.09

H.E.S.S. Crab nebula light curve

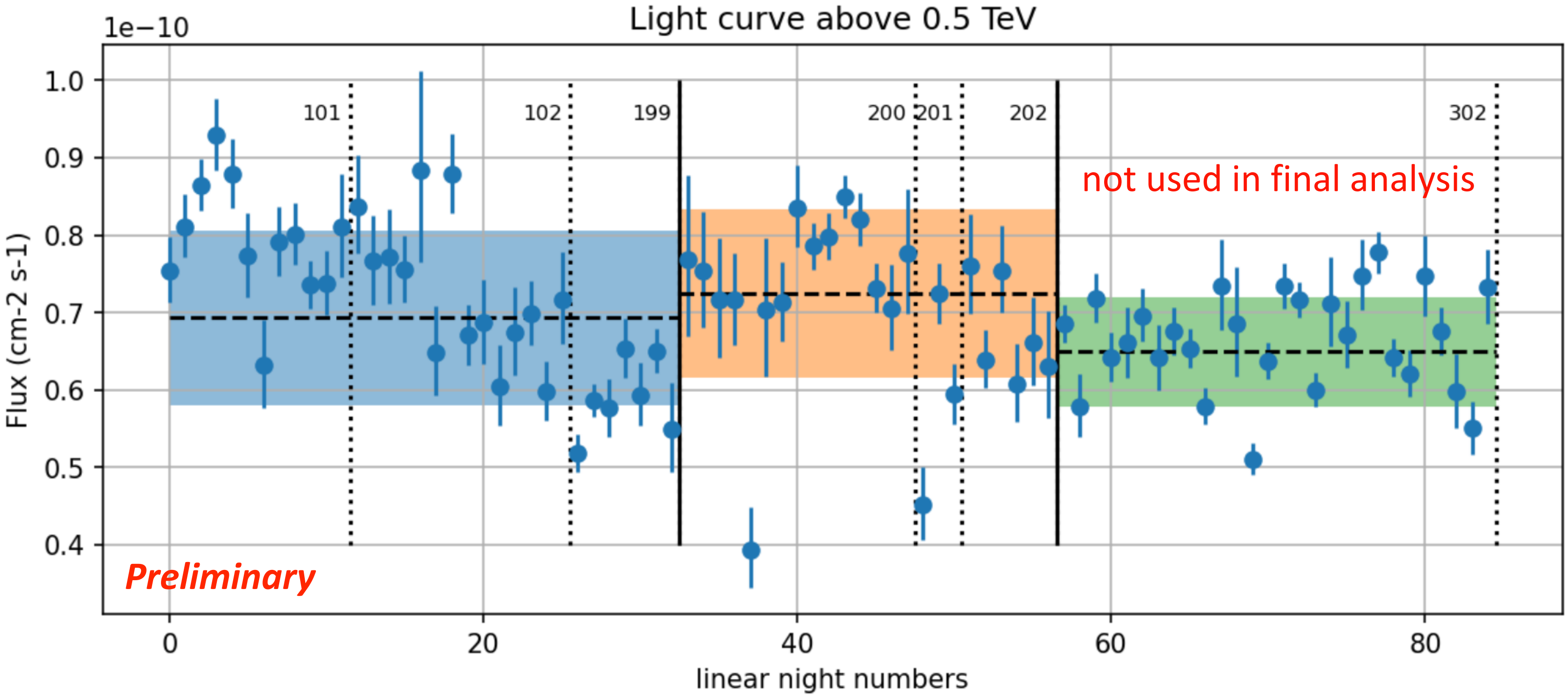

Combined fit — best-fit parameters

- Spectrum: smoothly broken power law $\frac{dN}{dE} = N_0 \left(\frac{E}{E_0}\right)^{-\Gamma_1} \left(1 + \frac{E}{E_{\text{break}}}^{\frac{\Gamma_2-\Gamma_1}{\beta}}\right)^{-\beta}$
- $E_0 = 1\,\text{TeV}$ fixed
- $N_0 = (4.7 \pm 0.5) \times 10^{-10}\,\text{TeV}^{-1}\,\text{s}^{-1}\,\text{cm}^{-2}$,
  $\Gamma_1 = 1.57 \pm 0.02$, $\Gamma_2 = 3.22 \pm 0.03$, $E_{\text{break}} = 0.64 \pm 0.06\,\text{TeV}$, $\beta = 3.01 \pm 0.12$
- Spatial model: Gaussian
- Best-fit position for whole energy range:
  $l = (184.5499 \pm 0.0004_{\text{stat}})^\circ$, $b = (-5.7825 \pm 0.0004_{\text{stat}})^\circ$
  (galactic coordinates, statistical uncertainties only)

Best-fit positions

- Best-fit positions in energy bands consistent within errors
- Best-fit position of global fit separated by 28'' from pulsar

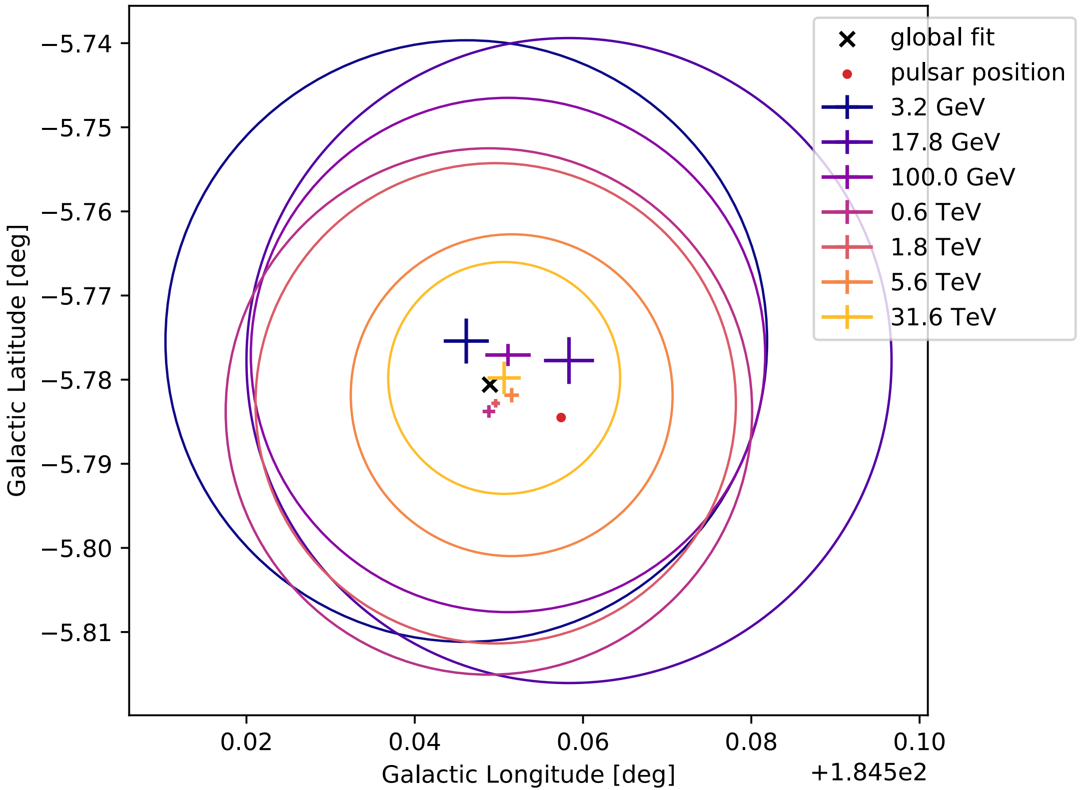

Best-fit model parameters

Parameter	variable B-field model	constant B-field model	Kennel & Coroniti
$\ln(n_{r,0})$	117.170	117.69	118.766
$\ln(\gamma_{r,\min})$	3.09 (fixed)	3.09 (fixed)	3.09 (fixed)
$\ln(\gamma_{r,\max})$	11.599	12.35	12.625
s_r	−1.5439	−1.649	−1.7419
ρ_r [″]	88.3	80.40	88.64
$\ln(n_{w,0})$	76.822	76.8315	−27.625
$\ln(\gamma_{w,\min})$	12.841	12.69	12.8366
$\ln(\gamma_{w,1})$	15.26	14.24	—
$\ln(\gamma_{w,2})$	19.197	19.35379	17.96
$\ln(\gamma_{w,\max})$	22.115	22.371	22.251
$\beta_{\min}$	2.8 (fixed)	2.8 (fixed)	2.8 (fixed)
$\beta_{\max}$	2 (fixed)	2 (fixed)	2 (fixed)
$s_{w,1}$	−3.117	−2.75	—
$s_{w,2}$	−3.3928	−3.1764	−2.8695
$s_{w,3}$	−3.782	−3.5118	−2.316
$\rho_{w,0}$ [″]	98.14	78.94	—
α_w	0.12544	0.11973	—
B_0 [μG]	256.4	126.39	—
r_{shock} [″]	13.4 (fixed)	13.4 (fixed)	13.4 (fixed)
α	−0.4691	—	—
σ	—	—	0.021396
$\ln(L_{\text{spin-down}}[\text{erg/s}])$	—	—	88.716
$r_{\text{dust,in}}$ [pc]	0.55 (fixed)	0.55 (fixed)	0.55 (fixed)
$r_{\text{dust,out}}$ [pc]	1.53 (fixed)	1.53 (fixed)	1.53 (fixed)
$\log_{10}(M_1/M_\odot)$	−4.4 (fixed)	−4.4 (fixed)	−4.4 (fixed)
$\log_{10}(M_2/M_\odot)$	−1.2 (fixed)	−1.2 (fixed)	−1.2 (fixed)
T_1 [K]	149 (fixed)	149 (fixed)	149 (fixed)
T_2 [K]	39 (fixed)	39 (fixed)	39 (fixed)

Relation to recent work by Dirson & Horns

- "Phenomenological modelling of the Crab Nebula's broadband energy spectrum and its apparent extension" — Dirson & Horns 2023, A&A **671**, A67
- Our "variable B-field model" is very similar to their model
- We use the same synchrotron data set in our fit
- Main difference in IC domain:
  - Dirson & Horns used published flux points & extension measurements
  - We fit to our combined *Fermi*-LAT and H.E.S.S. data

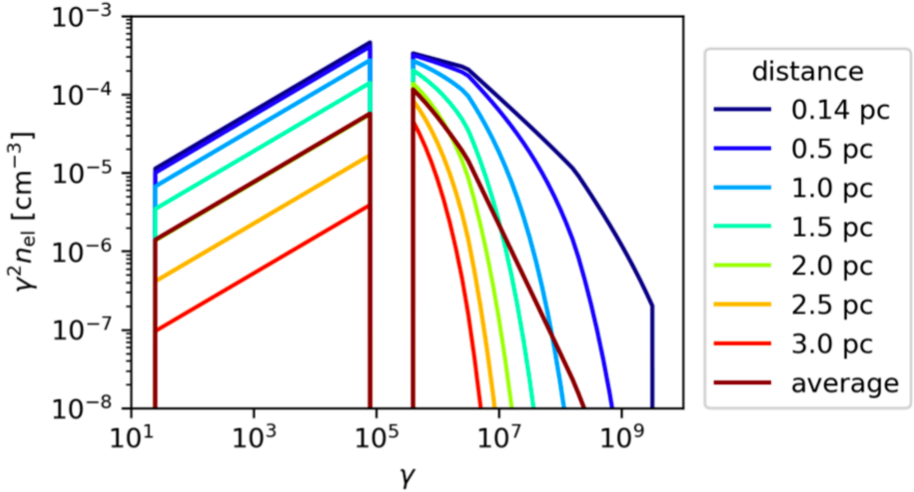

Relation to recent work by Dirson & Horns

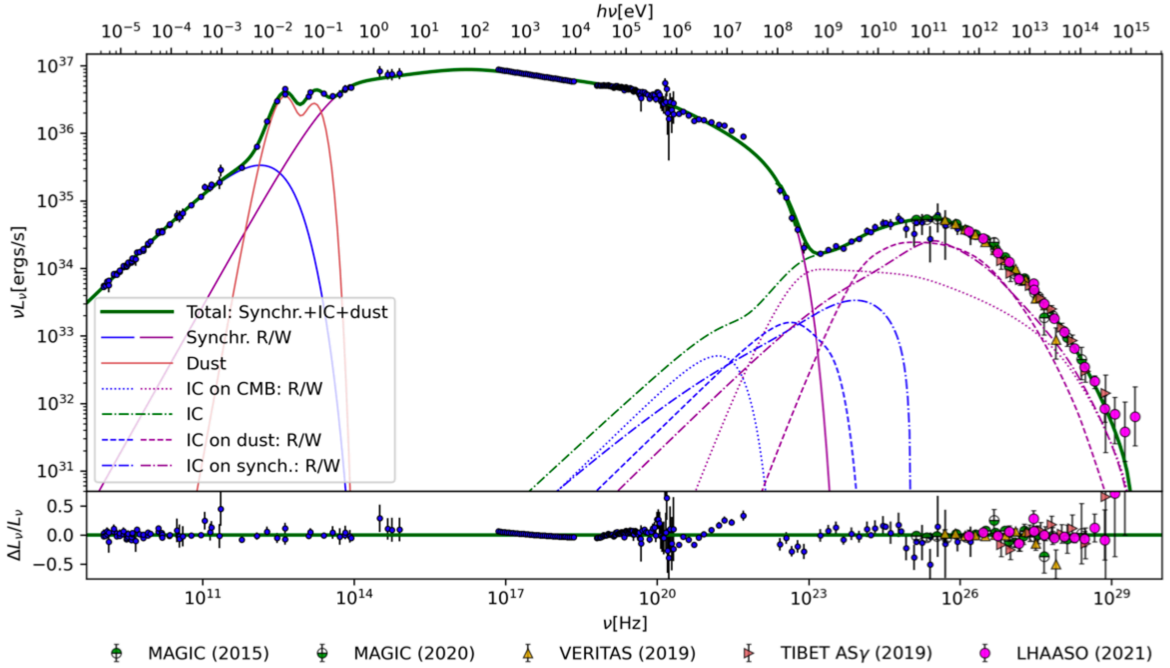

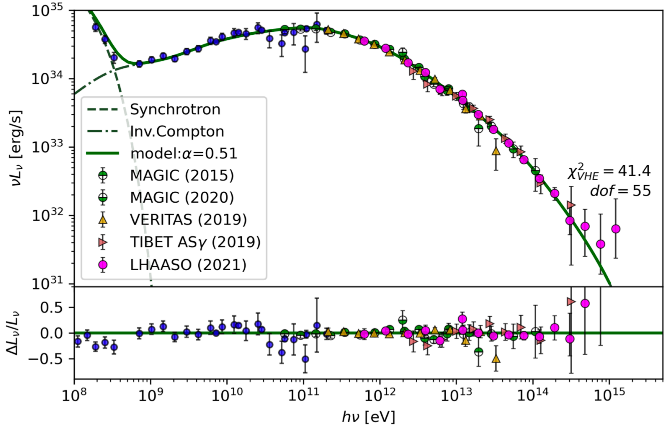

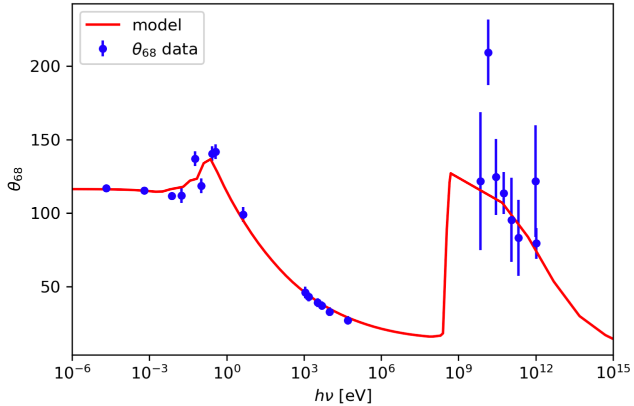

- Allowing for energy scale factors between experiments, they find a good fit of their model

Best-fit model parameters of Dirson & Horns

- Reference: Dirson & Horns 2023, A&A **671**, A67

Parameter	Best-fitting values (68% c.l.)
Radio electrons	
$\Psi_1 = s_r$	1.54 ± 0.03
$\Psi_2 = \ln(N_{r,0})$	114.7 ± 0.2
$\Psi_3 = \ln(\gamma_1)$	11.4 ± 0.1
$\Psi_4 = \rho_r$ [″]	89 ± 3
Wind electrons	
$\Psi_5 = s_1$	3.1 ± 0.2
$\Psi_6 = s_2$	3.45 ± 0.01
$\Psi_7 = s_3$	3.77 ± 0.04
$\Psi_8 = \ln(\gamma_{w0})$	12.7 ± 0.2
$\Psi_9 = \ln(\gamma_{w1})$	15.6 ± 0.8
$\Psi_{10} = \ln(\gamma_{w2})$	19.2 ± 0.2
$\Psi_{11} = \ln(\gamma_{w3})$	22.3 ± 0.03
$\Psi_{12} = \ln(N_{w,0})$	73.8 ± 0.5
$\Psi_{13} = \beta$	0.15 ± 0.01
$\Psi_{14} = \rho_0$[″]	99 ± 4

Dust parameters	
$\Psi_{15} = r_{\text{out}}$ [pc]	1.53 ± 0.09
$\Psi_{16} = \log_{10}(M_1/M_\odot)$	-4.4 ± 0.1
$\Psi_{17} = \log_{10}(M_2/M_\odot)$	-1.2 ± 0.1
$\Psi_{18} = T_1$ [K]	149 ± 8
$\Psi_{19} = T_2$ [K]	39 ± 2
Magnetic field parameters	
$\Psi_{20} = B_0$ [μG]	264 ± 9
$\Psi_{21} = \alpha$	0.51 ± 0.03
Goodness of fit	
$\chi^2_{\text{sync,SED}}$(d.o.f.)	182 (184)
$\chi^2_{\text{sync,ext}}$(d.o.f.)	16 (15)
$\chi^2_{\text{IC,SED}}$(d.o.f.)	22 (23)
$\chi^2_{\text{IC,ext}}$(d.o.f.)	24 (8)
χ^2_{VHE}(d.o.f.)	41 (55)
χ^2_{tot}(d.o.f.)	285 (285)